Fibroblast growth factor 9 is a novel modulator of negative affect

Elyse L. Aurbach, Edny Gula Inui, [...], and Huda Akil

SIGNIFICANCE

Molecular mechanisms mediating negative emotion and contributing to major depression remain elusive: here, we present evidence implicating fibroblast growth factor 9 (FGF9) as a key mediator. We use whole-transcriptome studies of postmortem human tissue to demonstrate that FGF9 is elevated in depression. Reverse translation animal studies demonstrate that both endogenous and exogenous FGF9 promotes anxiety- and depression-like behavior. Conversely, localized blockade of endogenous FGF9 expression decreases anxiety behavior. To our knowledge, this paper is the first description of hippocampal FGF9 function and the first evidence implicating FGF9 in negative affect. Thus, FGF9 represents a novel target for treating affective disorders. Moreover, our findings suggest that FGF2 and FGF9 work in functional opposition; we hypothesize that the balance between FGF factors may prove critical for optimal regulation of mood.

Keywords: fibroblast growth factor 9, major depression, anxiety, hippocampus, affect

ABSTRACT

Both gene expression profiling in postmortem human brain and studies using animal models have implicated the fibroblast growth factor (FGF) family in affect regulation and suggest a potential role in the pathophysiology of major depressive disorder (MDD). FGF2, the most widely characterized family member, is down-regulated in the depressed brain and plays a protective role in rodent models of affective disorders. By contrast, using three microarray analyses followed by quantitative RT-PCR confirmation, we show that FGF9 expression is up-regulated in the hippocampus of individuals with MDD, and that FGF9 expression is inversely related to the expression of FGF2. Because little is known about FGF9's function in emotion regulation, we used animal models to shed light on its potential role in affective function. We found that chronic social defeat stress, an animal model recapitulating some aspects of MDD, leads to a significant increase in hippocampal FGF9 expression, paralleling the elevations seen in postmortem human brain tissue. Chronic intracerebroventricular administration of FGF9 increased both anxiety- and depression-like behaviors. In contrast, knocking down FGF9 expression in the dentate gyrus of the hippocampus using a lentiviral vector produced a decrease in FGF9 expression and ameliorated anxiety-like behavior. Collectively, these results suggest that high levels of hippocampal FGF9 play an important role in the development or expression of mood and anxiety disorders. We propose that the relative levels of FGF9 in relation to other members of the FGF family may prove key to understanding vulnerability or resilience in affective disorders.

The neurotrophic hypothesis of major depressive disorder (MDD) posits that the neurobiological basis for mood disorders may be due to the dysregulation of growth factors and their effects on brain circuitry (1, 2). This hypothesis is supported by gene expression profiling experiments in postmortem human brains that implicate the fibroblast growth factor (FGF) family and other neurotrophins in MDD (3, 4). To date, only a few growth factors involved in mood disorders, such as brain-derived neurotrophic factor (BDNF) and FGF2, have been studied extensively.

Our laboratory and others have demonstrated that FGF2 is down-regulated in the frontal cortices (3), hippocampus (5), and locus coeruleus (4) in depressed individuals. This consistent decrease in FGF2 expression across regions is striking and underscores the likely importance of FGF2 in mediating affect.

Follow-up studies from our laboratory and others have focused on the FGF family and have demonstrated a key role of FGF2 in the control of emotional behavior. Rats exposed to chronic social defeat stress, an animal model recapitulating some aspects of MDD, showed decreased hippocampal FGF2 expression relative to unstressed controls (6), whereas subchronic and chronic administration of FGF2 had antidepressant properties (7, 8). Moreover, administration of antidepressants and anxiolytics induced FGF2 expression (9–11), and recent studies suggested that this induction is necessary for the effectiveness of the antidepressants (8). Paralleling the human depression studies, hippocampal FGF2 was basally decreased in high-anxiety animals, but chronic administration in adulthood (12) or a one-time administration of FGF2 during early development (13) alleviated their anxious phenotype. Additionally, anxiety-like behavior in outbred rats was increased by knocking down FGF2 in the dentate gyrus (DG) of the hippocampus (14). Collectively, these studies show that FGF2 is an endogenous anxiolytic and

antidepressant that plays both an organizational role during development and an ongoing role during adulthood to modulate emotional reactivity. The clinical relevance of FGF2 is further supported because its role in MDD was first discovered in the human brain (3).

Other members of the FGF family showed different patterns of dysregulation in postmortem tissue from individuals with MDD. Most notably, FGF9 had a pattern of dysregulation opposite to FGF2: FGF9 expression was increased in the frontal cortices (3) and locus coeruleus (4) in patients with MDD. This relationship is intriguing because additional evidence suggests that FGF2 and FGF9 may be functionally opposed. For example, FGF2 expression was decreased and FGF9 expression was increased in an in vitro cellular model of chronic stress (15).

Despite the evidence that FGF9 is altered in MDD, little is known about the function of this molecule in the brain. FGF9 is primarily expressed by neurons in the cortex, hippocampus, thalamus, cerebellum, and spinal cord (16–20), although it is also expressed by glia in the hindbrain and spinal cord (21). FGF9 interacts with several of the tyrosine kinase FGF receptors (FGFR) (22), binding preferentially to FGFR3 (23). Functionally, the literature suggests that FGF9 may promote cell survival. For example, FGF9 acts as a survival factor for nigrostriatal and mesencephalic dopamine neurons (24), and FGF9 treatment can increase the survival and soma size of cultured basal forebrain cholinergic neurons (25). FGF9 also weakly promoted proliferation and survival of cultured adult subventricular neural progenitor cells, inhibiting astrocyte differentiation (26). However, these are all studies of exogenous FGF9, which may be mimicking the actions of other FGFs. Moreover, none of the studies to date have examined the role of FGF9 in the hippocampus or its role in the regulation of emotionality.

Here, we specifically sought to elucidate the potential role of hippocampal FGF9 in the regulation of emotions and mood, given our early observations that FGF9 expression was altered in the postmortem hippocampus of individuals with MDD. We have carried out follow-up analyses in the human brain using multiple data sets to ascertain the relationship between FGF9 and other members of the FGF family. In addition, because it is difficult to determine whether gene dysregulation in postmortem human brain tissue contributes to the development of MDD or is a result of the disease process, we used a series of animal experiments to examine the role of FGF9 in affective behavior. To this end, we examined the effects of psychosocial stress, an animal model recapitulating some aspects of depression, on hippocampal FGF9 expression. We also characterized the effects of FGF9 administration and knockdown on anxiety-like and depression-like behavior and hippocampal gene expression. The combination of these various strands of evidence provides strong support for FGF9 as an endogenous molecule that promotes negative affect and may play a role in vulnerability to major depression.

RESULTS

Human Studies.

FGF9 expression was increased in the hippocampus of depressed individuals. Based on published data indicating that specific growth factor transcripts are altered in depressed brains (3–5), we selectively examined their differential expression in major depression using three human hippocampal microarray datasets. We examined diagnosis-related gene expression using a linear model that controlled for a variety of confounding pre- and postmortem variables and found that hippocampal FGF9 expression was consistently increased in subjects with MDD relative to controls in all three datasets, across platforms (Table 1). Using quantitative real-time polymerase chain reaction (qRT-PCR), we confirmed that FGF9 expression was increased by 32% in individuals with MDD relative to controls, with a Cohen's *d* effect size of 0.57, a medium-sized effect (Table 1). In the microarray data, FGFR1 and FGFR2 appeared to be down-regulated in individuals with MDD, but these effects were borderline significant and platform-specific (Table S1). Expression of BDNF, glial-derived neurotrophic factor (GDNF), FGF2, and FGFR3 did not differ in MDD subjects relative to controls (Table S1). Thus, these analyses pointed to FGF9 as one of the most clearly and consistently altered growth factors in MDD: we always observed it to be up-regulated in the depressed hippocampus.

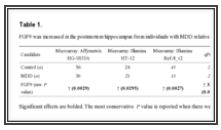

Table 1.

FGF9 was increased in the postmortem hippocampus from individuals with MDD relative to nonpsychiatric controls

Table S1.

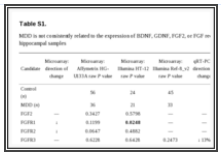

MDD is not consistently related to the expression of BDNF, GDNF, FGF2, or FGF receptors in our postmortem hippocampal samples

FGF9 expression is correlated with expression of other members of the FGF family. We further explored whether the relationship between the expression of hippocampal FGF9 and other candidate members of the FGF family differed by diagnosis (Fig. 1 *A–D*). We found that the expression of FGF9 was significantly negatively related to FGF2, FGFR1, FGFR2, and FGFR3. A negative correlation between FGF9 and FGFR1 was present in MDD but not in control tissue (Fig. S1*A*). These correlations suggest a general dysregulation in the FGF system in MDD, with FGF9 appearing to be one of the key players.

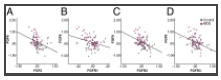

Fig. 1.

Postmortem hippocampal FGF9 expression correlates with expression of other FGFs. FGF9 expression in postmortem hippocampal tissue is negatively correlated with expression of (*A*) FGF2 ($R^2 = 0.15$, $P < 0.001$), (*B*) FGFR1 ($R^2 = 0.09$, $P < 0.001$), ...

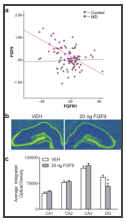

Fig. S1.

The relationship between FGF9 and FGFR1 is altered in postmortem hippocampal tissue from individuals with MD, and chronic FGF9 administration alters expression of FGFR1 in rats. (*A*) FGF9 expression negatively correlated with FGFR1 expression in the postmortem ...

Animal Studies.

Repeated social stress increased both social avoidance behavior and FGF9 gene expression. We subjected rats to repeated social stress over 10 days. Rats subjected to the stress paradigm showed significantly less weight gain during the experiment (Fig. S2 *A* and *B*) compared with handled controls. These stressed rats also showed increased social avoidance behavior in the social interaction test (Fig. 2*A*). Hippocampal FGF9 mRNA expression was significantly increased following repeated social stress compared with handled controls (Fig. 2 *B* and *C*); we observed this increase by tracing hippocampal subregions CA1, CA2, CA3, and dentate gyrus from mRNA in situ hybridization (ISH) autoradiograms (*Materials and Methods*). Thus, this model replicated the observations in the human MDD brain.

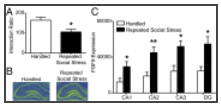

Fig. 2.

Social defeat stress increases FGF9 expression in the rat hippocampus. (*A*) Rats subjected to repeated social stress showed increased social avoidance [$t(17) = 2.5$, $P < 0.03$; $n = 8–10$ animals per group]. (*B*) Representative pseudocolored ...

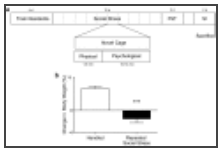

Fig. S2.

Social defeat experiment. (*A*) Timeline of the repeated social stress experiment. (*B*) Rats subjected to repeated social stress had a significant reduction in body weight, indicative of increased stress compared with vehicle controls [$t(22) = 5.8$, $P < ...$

Chronic FGF9 microinjections increased both anxiety-like and depression-like behavior. We performed a dose-finding study by acutely administering FGF9 or vehicle (intracerebroventricular, i.c.v.) to examine the effect of exogenous FGF9 on spontaneous affective behavior. We administered a range of doses over five orders of magnitude (Fig. S3 *A–C*): of these, we found that 20 ng FGF9 altered both anxiety- and depression-like behavior acutely, so we chose to use this dose to determine whether long-term exposure to FGF9 was sufficient to alter spontaneous affective behavior. Chronic FGF9 administration increased anxiety-like behavior on the elevated plus maze (EPM). FGF9-microinjected animals spent less percent time in the open arms of the EPM compared with vehicle controls (Fig. 3*A*). We observed a decrease

in the percent time spent climbing and an increase in the percent time spent immobile in animals injected with FGF9 compared with vehicle controls on the forced swim test (FST) (Fig. 3*B*). Chronic FGF9 microinjections did not alter locomotor activity (Fig. S3*D*), indicating that the effects were specific to affective-like behavior. Chronic FGF9 administration also decreased FGFR1 expression in the dentate gyrus (Fig. S1 *B* and *C*).

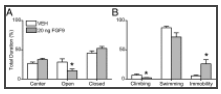

Fig. 3.

FGF9 administration altered anxiety- and depression-like behavior in rats. (*A*) Chronic FGF9 microinjections increased anxiety-like behavior as evidenced by a decrease in the percent time spent on the open arm compared with vehicle controls [$F_{(1,16)}$ = ...

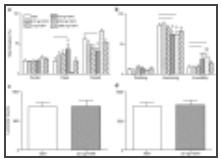

Fig. S3.

(*A*) An acute microinjection of FGF9 decreased anxiety-like behavior in an inverted-U dose–response curve, as shown by an increase in the percent time spent on the open arm and decreased closed arm time compared with vehicle controls [$F_{(5,58)}$ = ...

Animals administered LVshFGF9 had significantly less FGF9 expression in the dentate gyrus relative to LVshNS. To determine whether endogenous FGF9 expression was necessary for the expression of affective behavior, we used a lentiviral vector that used RNA interference to knock down expression of FGF9 (Fig. S4). Four weeks after microinjecting the knockdown (LVshFGF9) or control (LVshNS) viruses bilaterally into the dentate gyrus, we assessed effects on behavior and euthanized all animals (Fig. S5*A*). We confirmed the impact of the localized viral injection by examining enhanced green fluorescent protein (eGFP) expression, a marker for successful viral transduction, with concurrent changes in FGF9 expression in the dentate gyrus. Animals who received the LVshFGF9 knockdown virus showed significantly less FGF9 expression relative to LVshNS control animals, indicating that LVshFGF9 was successful in reducing FGF9 expression by ~30% (Fig. 4 *A* and *B*). In contrast, when we examined expression of other members of the FGF family, we found no effect of FGF9 knockdown (Fig. S5 *B*–*E*). Therefore, the LVshFGF9 virus was both effective and selective in reducing FGF9 expression in the dentate gyrus.

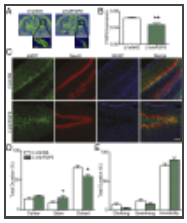

Fig. 4.

Lentiviral-mediated FGF9 knockdown reduced FGF9 expression in dentate granule neurons and decreased anxiety-like behavior. (*A*) Representative pseudocolored autoradiograms from mRNA in situ hybridization against FGF9 for animals transduced with a control, ...

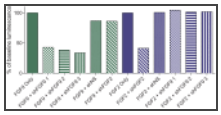

Fig. S4.

FGF9 shRNA constructs effectively and selectively knock down expression of FGF9 in vitro. shRNAs targeted against FGF9 (three candidates: shFGF9 1, shFGF9 2, shFGF9 3), FGF2 (shFGF2), and a control, nonsilencing construct (shNS). COS7 cells were transfected ...

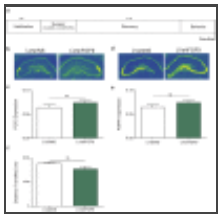

Fig. S5.

Knocking down FGF9 expression does not affect expression of FGF2 or FGFR1, and knocking down FGF9 selectively impacts anxiety-like behavior. (*A*) Experimental schema for in vivo FGF9 knockdown experiments. (*B* and *C*) Representative pseudocolored autoradiograms ...

The LVshFGF9 and LVshNS viruses primarily infected dentate granule neurons. To examine the cell types impacted by lentiviral infection, we performed triple-label immunohistochemistry, using antibodies against eGFP to mark transduced cells, NeuN to label neurons, and GFAP to identify astrocytes. We observed that the vast majority of colocalization occurred between eGFP and NeuN, with very few GFAP-labeled

cells showing concurrent eGFP expression (Fig. 4*C*). The pattern of transduction and colocalization did not differ between LVshNS and LVshFGF9 animals. Therefore, the virus preferentially transduced dentate granule neurons, suggesting that the behavioral effects of FGF9 knockdown are likely mediated through these cells.

FGF9 knockdown decreased spontaneous anxiety-like behavior on the EPM. Only animals who expressed eGFP in the dentate gyrus bilaterally in at least four serial sections were included, leaving 8 animals per group. LVshFGF9 animals spent significantly less time in the closed arms of the EPM than did LVshNS control animals (Fig. 4*D*), suggesting an anxiolytic effect. Similarly, LVshFGF9 animals spent more time in the open arms than did LVshNS animals, although this trend did not reach statistical significance (Fig. 4*D*). The impact of FGF9 knockdown was selective to anxiety-like behavior: we observed no differences between groups in the total distance traveled (Fig. S5*F*). There were no differences in depression-like behavior on the FST (Fig. 4*E*).

DISCUSSION

This series of studies is the first, to our knowledge, to link the dysregulation of hippocampal FGF9 to affective disorders. Using microarray data from several analyses with qRT-PCR validation, we showed that FGF9 expression is increased in the postmortem hippocampus of individuals diagnosed with MDD relative to nonpsychiatric controls. We demonstrated that FGF9 expression is negatively correlated with FGF2 expression, as well as with three FGF receptors (FGFR1, FGFR2, and FGFR3). To address the functional significance of these observations in human brain, we performed a complementary series of experiments in a rodent model to better characterize the role of FGF9 in affective processes. Chronic social defeat stress decreased social interaction and body weight in our animals and was associated with increased hippocampal FGF9 expression. Chronic FGF9 administration increased both anxiety- and depression-like behavior. Conversely, knocking down FGF9 expression in the dentate gyrus decreased anxiety-like behavior. These animal studies provide converging, complementary evidence for the role of FGF9 as an anxiogenic and prodepressant agent in the rodent brain. Together, this body of work suggests that FGF9 is an endogenous factor that enhances vulnerability to negative affect. Indeed, we believe that FGF9 is the first growth factor to be described as having a sustained anxiogenic and prodepressant role in the hippocampus. Thus, an agent that blocks the effects of FGF9 may be useful in treating human affective disorders.

FGF9 Expression Is Dysregulated in the Postmortem Hippocampus from Individuals Diagnosed with MDD. Using microarray and qRT-PCR, we observed a significant increase in hippocampal FGF9 expression in individuals with MDD. We did not observe a decrease in BDNF, GDNF, or FGF2 expression. In previous studies, other groups have observed a decrease in hippocampal FGF2 expression in depressed patients using mRNA ISH (5). The reason behind the discrepancy in our results is not clear, but may be due to differences in technique (microarray vs. mRNA ISH) or because tissue pH was higher in our study, and low pH can impact gene expression (27). Moreover, factors such as comorbid anxiety or a treatment history that includes antidepressant drugs would likely influence these transcripts, and we could not fully account for these factors.

We uncovered a significant negative correlation between hippocampal FGF9 expression and FGF2 expression in postmortem hippocampal tissue, and this relationship may indicate that these transcripts work in functional opposition. In support of this idea, we have previously observed contrasting patterns of FGF2 and FGF9 expression in other brain regions from individuals diagnosed with MDD. Specifically, FGF2 expression was reduced and FGF9 expression was elevated in the frontal cortices (3) and locus coeruleus (4) of the depressed brain relative to controls. The negative correlations between FGF9 expression and other FGFs also underscore the biological significance of FGF9 dysregulation in affective disorders: these relationships indicate that FGF9 may be acting in a complex network of molecules, and the alterations in FGF9 expression are concurrent with changes in other FGF family members that we have previously observed to impact affective behavior. However, these human studies are, by nature, correlational, and do not address whether these changes are a by-product of an underlying pathology associated with MDD or if they are part of the disease process. Moreover, many of the patients had a treatment history including antidepressants and/or other psychoactive drugs. Both the clinical and the toxicology data revealed a great deal of heterogeneity in drug exposure, making it difficult to analyze the impact of these drugs on the expression of FGF9. Thus, it will be important for future animal studies to ascertain whether psychoactive drugs can modify the expression of FGF9. As noted above, such studies on FGF2 indicate that the dysregulation we observed in MDD is not secondary to these treatments, but occurs despite them: antidepressants induce FGF2 and mediate their actions in part through that induction. Whether antidepressants inhibit FGF9 expression remains to be ascertained.

FGF9 Expression Mediates Affect in an Animal Model. We previously demonstrated that hippocampal FGF2 expression is decreased in rats

subjected to 4 days of social defeat stress (6). We also found that hippocampal FGF2 expression correlates with variability in anxiety- and depression-like behavior. For example, endogenous hippocampal FGF2 expression correlated with spontaneous open arm time on the EPM in outbred rats (14). Moreover, animals that naturally exhibit high anxiety-like behavior have low levels of hippocampal FGF2 (12, 13). In contrast, we have demonstrated here that ten days of social defeat stress up-regulates hippocampal FGF9 expression while decreasing body weight and social interactions, correlates of increased depression-like behavior. These results are congruent with our observations from human studies and indicate that hippocampal FGF9 may play an important role in stress responsiveness.

Chronic administration of FGFs produced coordinate effects on anxiety- and depression-like behavior: FGF2 reduced anxiety- (12) and depression-like (7) behavior. In contrast, we demonstrate here that chronic FGF9 administration increases anxiety-like and depression-like behavior, demonstrating again that the two FGFs have opposing effects. Given that antidepressant and anxiolytic medications induce growth factor expression (9–11), it may be that administering growth factors directly activates the same physiological mechanisms as classical anxiolytics and antidepressants. Indeed, work from others indicates FGF2 is necessary for the positive effect of antidepressants (8). However, one limitation of our FGF9 administration studies is the lack of anatomical specificity: that is, that administration into the lateral ventricle likely affects many brain regions in addition to the hippocampus. Other regions, including the prefrontal cortices, are also likely to be involved in the behavioral expression of these changes in negative affect, and future studies can better elucidate the function of FGF9 in these regions.

Altering endogenous gene expression using transgenic mice or viral-mediated knockdown can be used to demonstrate that hippocampal growth factor expression is necessary for appropriate spontaneous regulation of affective behavior. We previously used a lentiviral vector to knock down FGF2 expression in the dentate gyrus of outbred rats, increasing anxiety-like behavior on the EPM (14). Similarly, knocking down hippocampal FGF2 eliminated basal behavioral differences in selectively bred rats that typically exhibit differences in spontaneous anxiety-like behavior (28). In contrast, we demonstrate here that using a lentiviral vector to knock down FGF9 expression bilaterally in the dentate gyrus decreases anxiety-like behavior. Interestingly, unlike the results of the administration experiments, our knockdown experiments have produced effects on anxiety-like, but not depression-like, behavior. These findings may result from several factors: (*i*) the magnitude of the knockdown: the degree of FGF9 knockdown (~30%) may not be sufficient to alter depression-like behavior; (*ii*) partial effect: FGF9 knockdown in the dentate gyrus may increase vulnerability to depression-like behavior, but stress exposure may be required to uncover behavioral changes; and/or (*iii*) anatomical specificity: our injections were highly localized to the dentate gyrus and had limited spread. This region may be critical to the regulation of anxiety behavior, but may be less pivotal in the control of depression-like behavior. Furthermore, FGF9 may play somewhat different roles in separate components of the negative affect circuitry, regulating anxiety in the dentate gyrus but depression-like behavior in other brain regions, including the prefrontal cortices and/or mesolimbic dopamine system. This hypothesis is quite plausible as we have previously observed effects exclusive to anxiety-like behavior after knocking down FGF2 expression selectively in the dentate gyrus (14, 28). Future studies can examine these possibilities.

It should be noted that MDD and anxiety disorders are often comorbid. Typically 75% of MDD patients exhibit comorbid anxiety (29). Our records document the existence of comorbid clinical anxiety in 58% of the MDD subjects. This figure is likely an underestimate due to the methods for psychological autopsy in our Brain Bank. Therefore, additional studies are needed to examine whether factors known to influence gene expression in MDD, including comorbid anxiety, impact hippocampal FGF9 expression. Further, it will be of interest to study the role of FGF9 in other brain regions implicated in MDD, including the prefrontal cortices and mesolimbic dopamine circuit. It may also be fruitful to more fully explore the impact of classical antidepressants on hippocampal FGF9 levels in postmortem human tissue, and animal studies involving antidepressant administration and other resilience-inducing manipulations (including environmental enrichment) can be used to clarify effects.

SUMMARY

We demonstrated here that FGF9 is an anxiogenic and prodepressant growth factor in the hippocampus. FGF9 expression was up-regulated in the postmortem hippocampus of individuals with MDD, and psychosocial stress, a model of depression in rodents, increased FGF9 gene expression. Chronically, exogenous FGF9 increased anxiety- and depression-like behavior, whereas knocking down endogenous FGF9 expression reduced anxiety-like behavior. These results contrast to a body of work indicating that high levels of hippocampal FGF2 may promote resilience (Table S2). Therefore, we hypothesize that FGF2 and FGF9 act as physiological antagonists to mediate emotionality and vulnerability to mood disorders. Together, this body of work suggests that blocking the actions of hippocampal FGF9 offers a novel

therapeutic approach to the treatment of anxiety and depression.

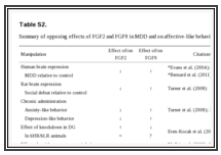

Table S2.

Summary of opposing effects of FGF2 and FGF9 in MDD and on affective-like behavior in rodents

MATERIALS AND METHODS

Human Studies.

Subject characteristics and tissue extraction. The human tissue samples used for all three microarray experiments and qRT-PCR validation were obtained from the Brain Donor Program at the University of California, Irvine, with the consent of the next of kin. Frozen coronal slabs were dissected to obtain hippocampal tissue samples (*SI Materials and Methods*), and total RNA was extracted using procedures described previously (27). Clinical information was obtained from medical examiners, coroners' medical records, and a family member. Patients were diagnosed by consensus based on criteria from ref. 30. For further information regarding data collection procedures, please see Li et al. (31). Final control and MDD sample sizes can be found in Table 1, and demographics are in Table S3. It should be noted that the control and MDD samples used for the three microarray studies and qRT-PCR overlap by 42–100% (Table S4), and thus the results can be best interpreted as showing strong technical replication at four different institutions, using three different microarray platforms, in addition to qRT-PCR.

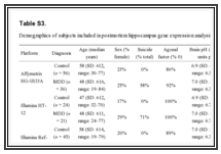

Table S3.

Demographics of subjects included in postmortem hippocampus gene expression analysis

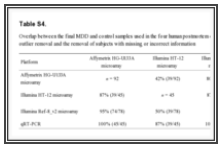

Table S4.

Overlap between the final MDD and control samples used in the four human postmortem experiments following outlier removal and the removal of subjects with missing or incorrect information

Gene expression profiling. In general, the labeling and hybridization of sample mRNA with oligonucleotide probes followed standard manufacturer protocols. Analyses used the full microarray datasets (all probe data from the MDD and control subjects, as well as from small samples of subjects with bipolar disorder and schizophrenia) to maximize our ability to identify technical artifacts and confounds, although the reported results focus exclusively on MDD vs. control comparisons for a subset of growth factor probes. As is traditional, all probe signal values were log (base 2)-transformed to reduce heteroskedasticity and quantile-normalized to remove technical artifacts in the overall distribution of signal per sample. For more detail on each microarray system (Affymetrix, Illumina HT-12, and Illumina Ref-8), preprocessing methods, and quality control, refer to *SI Materials and Methods*.

Microarray analysis: determining diagnosis-related gene expression while correcting for confounding variables. The degree of severity and duration of physiological stress at the time of death was estimated by calculating an agonal factor score (AFS) for each subject (32). Additionally, we measured the pH of cerebellar tissue as an indicator of the extent of oxygen deprivation experienced around the time of death (27). We also calculated the interval between the estimated time of death and the freezing of the brain tissue [the postmortem interval (PMI)] using coroner records. We ensured high quality data by choosing samples with relatively high pH and low agonal factor (Table S3), but still controlled for these variables, as well as age and sex, by including them as terms in our linear model

$$(probe\ signal) \approx \beta_0 + \beta_1(Brain\ pH) + \beta_2(Agonal\ Factor) + \beta_3(PMI) + \beta_4(Age) + \beta_5(Sex) + \beta_6(Diagnosis). \quad [1]$$

Within the Affymetrix microarray data, we further explored whether the relationship between FGF9, FGF2, and each of the FGF receptors

might be altered in MDD. First, to ensure that the relationships that we observed were not due to the major confounds present in the dataset, we reduced their influence using estimates of their effects provided by the model in Eq. **1** (*SI Materials and Methods*). This allowed us to examine the relationship between the FGF-related genes in data resembling that from subjects with consistent pre- and postmortem factors using the linear model

$$(\textit{cleaned probe signal for FGF9}) \approx \beta_1(\textit{cleaned probe signal for FGF2/R1/R2/R3}) + \beta_2(\textit{Diagnosis}) + \beta_3[(\textit{Diagnosis})* (\textit{cleaned probe signal for FGF2/R1/R2/R3})]. \quad [2]$$

qRT-PCR validation. Microarray results represent relative levels of probe signal, so we validated them using qRT-PCR. Total RNA (1 μg) was extracted, reverse transcribed, and run in duplicate in qRT-PCR assays as previously described (3, 33) (*SI Materials and Methods*). Expression of the gene of interest was normalized to β-actin.

Animal Studies.

Animal characteristics and housing. Adult male Sprague–Dawley rats (Charles River Laboratories), weighing between 220 and 350 g, were housed in pairs on a 12/12-h light/dark schedule, with access to food and water ad libitum. Additional housing details can be found in *SI Materials and Methods*. All experiments were conducted with approval of the University of Michigan Committee on the Use and Care of Animals.

Repeated social stress and FGF9 administration studies. To determine the effects of stress on FGF9 gene expression, we used a social stress paradigm consisting of repeated agonistic encounters with a territorial, aggressive rat. We assessed the behavioral and metabolic effects of social defeat using the social interaction test and by measuring the change in body weight (*SI Materials and Methods*). To determine whether FGF9 microinjections altered affective-like behavior, we performed a dose–response analysis of FGF9 administration. Under anesthesia, rats were implanted with a guide cannula in the left lateral ventricle (coordinates from bregma: AP −1.1; ML +1.3; DV −3.0) and given 5 d to recover. During the acute study, the rats were microinjected with either recombinant human FGF9 (0.2, 2, 20, 200, or 2000 ng; Cell Sciences) or vehicle [artificial extracellular fluid (AECF), with 100 μg/mL BSA]. Eight microliters was infused over 8 min, and 5 min was allowed for diffusion. The rats were tested 24 h later on day 2 of the forced swim test (FST; *SI Materials and Methods*). One week later, rats received another FGF9 microinjection 15 min before EPM testing. During the chronic study, rats were microinjected daily with FGF9 (20 ng, i.c.v.) or vehicle (AECF, i.c.v.) between 0800 and 1200 hours for 18 d, and animals were tested in the EPM (day 14) for locomotor activity (day 15) and in the FST (day 17 and day 18) (*SI Materials and Methods*) following microinjection, between 0800 and 1300 hours.

FGF9 knockdown in vitro and in vivo. We generated three 19-mer siRNA sequences targeted against the coding region of the rat FGF9 mRNA: FGF9 siRNA1 (AGGAAAGACCACAGCCGAT), FGF9 siRNA2 (GGAAAGACCACAGCCGATT), and FGF9 siRNA3 (GGACCAGGACTAAACGGCA). shRNA sequences were created by adding a loop sequence (UUCAAGAGA) and restriction enzyme sites. The shRNA constructs were synthesized (Invitrogen) and subcloned into the pLentiLox3.7 lentiviral vector, which contains an eGFP reporter tag. A nonsilencing shRNA (shNS) sequence was used as a control (14). shRNA3 was selected for use in vivo because it was most effective at reducing FGF9 expression in vitro (Fig. S4) and showed the least toxic effects on cultured cells (<10% cell death). The vector containing shRNA3 (hereafter referred to as shFGF9) and the shNS vector were submitted to the University of Michigan Viral Vector core for synthesis. The returned lentiviruses (100× concentration; LVshFGF9 and LVshNS) were used in FGF9 knockdown experiments in vivo.

All animals underwent microinjection surgery (groups: LVshFGF9, LVshNS). Under isoflurane anesthesia, a 33-gauge microinjector was lowered bilaterally just above the dentate gyrus of the hippocampus (coordinates from bregma: A/P −5.0, M/L ±3.5, D/V −3.6–3.8). One microliter of LVshNS or LVshFGF9 was infused over 4 min (14), and 2 min were allowed for diffusion. We allowed 4 wk for recovery, and then animals were subjected to behavioral testing in the EPM and FST (*SI Materials and Methods* and Fig. S5*A*).

Behavioral testing. We monitored locomotor activity for 1 h (*SI Materials and Methods*). We used the FST to determine examine depressive-like behavior (*SI Materials and Methods*). We used the EPM to examine anxiety-like behavior (*SI Materials and Methods*).

mRNA ISH. All rats were euthanized by rapid decapitation; brains were removed, snap-frozen, and stored at −80 °C. Ten-micrometer sections were taken every 200 μm through the hippocampus, and ISH methodology was performed as previously described (34) (*SI Materials and Methods*). All in situ probes were synthesized in-house, and exposure times were experimentally determined for optimal signal (*SI Materials and Methods*). mRNA expression signals from autoradiographic films were quantified using computer-assisted optical densitometry software,

Scion Image (Scio Corporation) or ImageJ (National Institutes of Health). For all experiments except FGF9 knockdown, integrated optical densities were determined by outlining a hippocampal subfield (CA1, CA2, CA3, and dentate gyrus) on each hemisphere, correcting for background. For quantification of sections from animals in the FGF9 knockdown study, we used a modified approach that enabled us to quantify expression of a gene target only with evidence of successful viral transduction (*SI Materials and Methods*). eGFP autoradiograms were also analyzed animal by animal: animals in the knockdown study were only included in the final behavioral analysis if they showed robust expression of eGFP in the dentate gyrus of both hemispheres in at least four adjacent sections (≥800 μm), without labeling of other structures. After exclusion, eight animals were included in each group.

Immunohistochemistry. Animals (n = 4 animals/group; LVshNS, LVshFGF9) underwent the same surgical procedures as above. Three weeks after surgery, animals were transcardially perfused using 4% (wt/vol) paraformaldehyde (PFA). Free-floating sections (45 μm) were blocked for 1 h at room temperature and incubated overnight at room temperature with chicken anti-GFP, 1:2,000 (Abcam); rabbit anti-NeuN, 1:300 (Abcam); and mouse anti-GFAP, 1:500 (Millipore). Sections were washed and transferred to secondary solution (AlexaFluor488 goat anti-chicken IgG, 1:200; AlexaFluor568 goat anti-rabbit IgG, 1:200; AlexaFluor 647 goat anti-mouse, 1:200; Life Technologies) for 2 h at room temperature. Sections were washed, mounted, and coverslipped using ProLong Gold Antifade Reagent with DAPI (Fisher Scientific). Slides were imaged on an Olympus Fluoview FV1000 confocal microscope (*SI Materials and Methods*).

Statistical analyses. Analysis of human data are described above. All animal behavioral tests were analyzed by one-way ANOVA or Student t test.

SI MATERIALS AND METHODS

Human Data.

Dissection of human hippocampus. For the first stage of dissection, a 1-cm coronal slab was placed on a block of dry ice. The hippocampus was visually identified using the dentate gyrus by an expert in human neuroanatomy, and a fine jeweler's blade in a coping saw handle was used to dissect the hippocampus and surrounding temporal cortex. Both sides of the slab were carefully inspected. In some cases, more than one slab was used to cover the full extent of the structure. The block was wrapped in foil, placed on dry ice, and then stored at −80 °C until further processing. The second stage of finer dissection was then carried out. The temporal cortex was removed by visual inspection using the dentate gyrus and CA3 as landmarks. The dissected tissue was then processed for RNA extraction.

Gene expression profiling.

Affymetrix microarray. Microarray experiments were performed in eight separate experimental cohorts containing both patients and controls. The majority of RNA samples were analyzed in duplicate at two different laboratories using Affymetrix Genechips (either U133A or U133Plus-v2). We extracted the U133A subset of probes and applied RMA (robust multiarray analysis) to summarize probe set expression levels using custom ENTREZ12.1 Chip Definition Files (CDF), which defined probe sets for 11,912 transcripts (as defined by ENTREZ in 03/2010) and 68 control probe sets. To ensure sample quality, we required an average sample to sample correlation coefficient (r) of 0.9, excluding 6 of 235 samples (2.6%). Batch effects due to cohort, laboratory, and platform were removed by median centering the data. Replicate samples were then averaged, and any subjects that were missing information were removed from the dataset (n = 8), leaving a final sample size of 129 unique subjects. For further information regarding the Affymetrix data preprocessing procedures, please see Li and colleagues (31).

After extracting summarized probe signal data from scanned microarray image files using proprietary software specific to the microarray company or, in the case of the Affymetrix dataset, RMA all downstream analyses were completed in the R statistical programming language. For all of the microarray experiments, as part of quality control subjects were verified to have gene expression typical of their reported sex using data from genes XIST, EIF1AY, RPS4Y1, UTY, USP9Y, NLGN4Y, NCRNA00185, TTTY15, KDM5D, CYorf15B, and DDX3Y.

Illumina microarrays. For both Illumina microarrays, we imported the scanned images of the hybridized chips into GenomeStudio microarray data analysis software (Illumina), which combined the signal measurements from the 20–30 beads associated with each probe into a single signal intensity measurement. GenomeStudio also provided a detection P value, which represents the confidence that a given transcript was expressed above background as defined by a group of negative control probes.

Illumina HT-12 microarray. RNA was processed and hybridized with the Illumina HT-12 v3 microarray beadchips. The original 47,217 probes on the chip were filtered to exclude probes that were not significantly expressed (detection $P < 0.05$) in at least nine samples (~10% of the subjects). Following this filtering, 26,589 probes remained (56%). These probes were reannotated using the Bioconductor R package *illuminaHumanv4.db* (last updated 16 October 2013). The median Pearson sample-sample correlation (r) was high (0.97) for the dataset. The seven samples that had a sample-sample correlation much lower than this were excluded (7.3% of 96 samples). Technical batch effects were corrected by including a batch term in the statistical model used to analyze diagnosis effects (see below). Outlier samples were defined as having a distribution (boxplot) of sample-sample correlations that was distinctly low (below the median 0.10 quantile sample-sample correlation for the entire dataset).

Illumina Ref-8 microarray. RNA was processed and hybridized with the Illumina HumanRef-8_V2 microarray beadchips. Initially, 666 samples representing six brain regions were randomly distributed across 85 microarray chips. Batch effect removal required first median centering the normalized expression levels for each transcript within each region and then median centered the signal data for each transcript within each of the 85 chips. Twenty-two samples were removed due to having distinctly low sample-sample correlations (3% of 666 samples). The 79 hippocampal samples were then extracted from the larger dataset. The original 22,177 probes on the chip were filtered to exclude probes that were not significantly expressed in the majority of these samples (a median detection $P < 0.055$), leaving 13,334 probes (60%). These probes were annotated using output from GenomeStudio (v2). Two subjects were removed from the analysis due to exhibiting sex chromosome gene expression incongruent with reported sex.

Microarray analysis: determining diagnosis-related gene expression while correcting for confounding variables. Although agonal factor, brain pH, PMI, and sex did not differ significantly by diagnosis, we found that it was necessary to control for these variables because they strongly correlated with the top principal components of variation in the data sets (PC1–4). We also controlled for the average age at the time of death, which sometimes varied significantly with diagnosis.

Examining whether diagnosis influences the relationship between the expression of FGF family genes. Within the Affymetrix microarray data, we explored whether the relationship between FGF9, FGF2, and each of the FGF receptors might be altered in MDD. First, to ensure that the relationships that we observed were not due to the major confounds present in the dataset, we reduced their influence using estimates of their effects provided by the model in Eq. **S1**

$$(cleaned\ probe\ signal) \approx (probe\ signal) - \beta_1(Brain\ pH\text{-}6.88) + \beta_2(Agonal\ Factor) + \beta_3(PMI\text{-}23.5) + \beta_4(Age\text{-}52) + \beta_5(Sex). \quad [S1]$$

In other words, the data were projected to the median brain pH of 6.88, PMI of 23.5 h, agonal factor of 0, age 52 y, and male sex. This approach allowed us to examine the relationship between the FGF-related genes in data resembling that from subjects with consistent pre- and postmortem factors using the linear model:

$$(cleaned\ probe\ signal\ for\ FGF9) \approx \beta_1(cleaned\ probe\ signal\ for\ FGF2/R1/R2/R3) + \beta_2(Diagnosis) + \beta_3[(Diagnosis)* (cleaned\ probe\ signal\ for\ FGF2/R1/R2/R3)]. \quad [S2]$$

We also ran our analyses on an uncleaned probe signal dataset and found similar, stronger relationships between FGF9 and other FGF family members. In the main text, we only reported the more conservative results from the data cleaned of confounds.

qRT-PCR. Total RNA (1 μg) was reverse transcribed using the iScript cDNA synthesis kit (Bio-Rad Laboratories) in a total reaction volume of 20 μL. cDNA (1 μL) was used as the template for real-time PCR assays with a MyiQ real-time PCR system (Bio-Rad Laboratories). The qPCR was conducted in duplicate using iQ SYBR Green Supermix, according to the manufacturer's instructions (Bio-Rad Laboratories). Sequences for the left primer (start) were as follows: *FGF9*: GGGGAGCTGTATGGATCAGA (1,201); *FGFR3*: CTTGTGCCTGGGGTGTTAGT (3,133), Sequences for the right primer (start) were as follows: *FGF9*: GTGAATTTCTGGTGCCGTTT (1,391); *FGFR3*: AAAGGCTCCCATCTTCAGGT (3,240). Relative expression of the gene of interest was normalized to β-actin expression in each sample. The expression level of the gene of interest was evaluated using the $2^{-(\Delta\Delta Ct)}$ method (33). The PCR product quality was monitored using post-PCR melt-curve analysis at the end of the amplification cycles.

Animal Data.

RNA extraction. After dissection, samples were stored at −80 °C before RNA extraction. The starting blocks of tissue weighed an average of 600 mg. Tissue was homogenized in TRIzol reagent and treated with chloroform. Samples were centrifuged to separate the suspended RNA

from other cellular materials, and the RNA was pelleted and washed with ethanol. All RNA pellets were resuspended in diethylpyrocarbonate-treated water. The average concentration after extraction was 0.7 μg/μL for an average of 420 μg of total RNA. One hundred micrograms of the total RNA was purified using the RNeasy kit (Qiagen); RNA quality was assessed using the Agilent 2100 Bioanalyzer, and quantity was determined using a spectrophotometer (A260). All RNA concentrations were adjusted to 1 μg/μL with DEPC-treated water before first-strand DNA synthesis.

qRT-PCR. Total RNA (1 μg) was reverse transcribed using the iScript cDNA synthesis kit (Bio-Rad Laboratories) in a total reaction volume of 20 μL. cDNA (1 μL) was used as the template for real-time PCR assays with a MyiQ real-time PCR system (Bio-Rad Laboratories). The quantitative PCR was conducted in duplicate using iQ SYBR Green Supermix, according to the manufacturer's instructions (Bio-Rad Laboratories). Primer sequences were as follows: FGF9: AGCTGCCATACTTCGACTTATCAGGATTCTGGCTGGTGGCCTGCGCGAGG; FGFR3: TCACCCAAACCGGCAGGTGCGATTTTGTTAACCCAGCGACGAACTTTCCG. Relative expression of the gene of interest was normalized to β-actin expression in each sample. The expression level of the gene of interest was evaluated using the $2^{-(\Delta\Delta Ct)}$ method and values for each gene were expressed as fold changes (33). The PCR product quality was monitored using post-PCR melt-curve analysis at the end of the amplification cycles.

Repeated Social Stress and FGF9 Administration Studies.

Animals. Adult male Sprague–Dawley rats (Charles River Laboratories), weighing between 220 and 250 g, were housed in pairs on a 12/12-h light/dark schedule, with access to food and water ad libitum. Animals were allowed to acclimate to the housing environment for 7 d before any experiments began. Animals used in the microinjection studies were housed in pairs until the surgery and were singly housed after surgery. Animals in the knockdown study were pair-housed until the surgery, singly housed for 3 d after surgery, and then returned to pair-housing. Housing procedures for the repeated social stress experiments are described below. All animals were treated in accordance with the National Institutes of Health *Guidelines on Laboratory Animal Use and Care* and in accordance with the guidelines set by the university committee on use and care of animals at the University of Michigan.

Repeated social stress. To determine the regulation of FGF9 gene expression following stress, we used a repeated social stress paradigm consisting of two phases, a training phase lasting 4 d, and a repeated stressor phase lasting 10 d. During both phases, Long–Evans male rats (400–450 g) were housed with ovariectomized female rats to increase their territorial response and aggressive behavior. During the daily 15-min social stress episode, Long–Evans females were first removed from the resident cage and an intruder Sprague–Dawley rat (250–300 g) was introduced. The intruder was allowed to move freely throughout the cage until an intense physical episode occurred (1–5 min). After an initial physical attack, intruders were placed in a protective wire mesh cage (30 × 15 × 15 cm) and back into the residents' home cage for the remainder of the 15-min trial. This paradigm allowed for intense visual, auditory, and olfactory interactions emphasizing the psychosocial component of the stress while maintaining the physical safety of the intruder rat. After the 15-min social stress period, intruders were returned to their home cage and were singly housed. The female Long–Evans rats were returned to the cage of the resident. The intruders and residents were housed in different rooms throughout the entirety of the experiment. During the training phase (4 d), Long–Evans residents (n = 15) were trained to attack nonexperimental Sprague–Dawley intruders and were included when latency to attack was less than 1 min. Residents (n = 2) that were not included in the experimental group were used as novel resident targets in the social interaction test. During the repeated stressor phase (10 d), intruders were placed in a cage with a novel resident every day for 15 min during the dark phase of the light cycle between 1900 and 2200 hours. Control animals were placed in a novel cage and allowed to move freely for the 15-min period. Body weights were measured on day 1 of the repeated social stress and on day 10 following the last stress period.

Social interaction test. To determine whether repeated social stress caused any behavioral differences in the intruder rats compared with their nonstressed handled controls, we used a measure of social interaction (SI). The modified social interaction testing arena consisted of a black Plexiglas open field (100 × 100 cm) with boundaries marked for interaction zones and a target field. The movement of the Sprague–Dawley intruder rat was recorded by a video tracking system (Noldus Ethovision). The test consisted of two 5-min trial periods on consecutive days. Animals were assessed with without a novel resident Long–Evans rat present on day 1 and with the resident present on day 2. On day 1, the intruder was placed in the center of the testing field with no target. The second trial, 24 h later, consisted of 5 min during which the intruder rat was placed in the center of the test field with a caged resident present. The interaction ratio was calculated as 100 × (interaction time, target present)/(interaction time, target absent). Animals with a low social interaction ratio had increased social avoidance behavior (Fig. 2*A*).

Locomotion testing. The rats were placed in a 43 × 21.5 × 25.5-cm acrylic cage with stainless steel floor gridding. Horizontal and vertical

locomotor activity was monitored every 5 min for 1 h by two panels of photocells that recorded beam breaks. The horizontal and vertical components were added together and an average was found for each animal and group. The locomotion-testing rig and motion-recording software were developed in-house at the University of Michigan. All locomotor testing took place between 0800 and 1200 hours.

FST. We used the FST to determine effects on depression-like behavior. Day 1 consists of a 10- to 15-min pretest swim and day 2 is a 5-min test swim that provides valuable information on the animals' reaction to the second day of stress. Animals were placed in cylinders filled with water at a depth at which the rats' tail could not touch the bottom and a temperature of 25–27 °C. Immediately following the day 1 pretest, animals were dried, returned to their home cage, and injected with FGF9 (0.2, 2, 20, 200, or 2,000 ng, i.c.v.) or vehicle (AECF, i.c.v.). Water was changed between animals, and all sessions were recorded by a video camera. All FST swim sessions took place between 0900 and 1300 hours. The videotaped behaviors were scored by an observer blind to the experimental conditions. Swimming consisted of horizontal movement throughout the cylinder. Climbing was defined by vertically directed movement of forepaws against the wall of the cylinder. Immobility was defined as floating or the minimal movement necessary to keep the head above water level. Percent total duration of swimming, climbing, and immobility episodes was scored using The Observer software (Noldus Information Technology).

EPM. We used the EPM to determine effects on anxiety-like behavior. The EPM consists of black Plexiglas with four elevated arms (70 cm from the floor, 45 cm long, and 12 cm wide). The EPM has two arms enclosed by a 45-cm-high wall and two open arms arranged in the shape of a cross. At the intersection of the four arms of the maze, a 12 × 12-cm square platform allowed access to all four arms. During the 5-min test period, the room is dimly lit (~40 lx), and behavior is monitored using a computerized video tracking system (Noldus Ethovision). At the start of the 5-min test, the rat was placed in the center square platform. The tracking system recorded the latency to enter the open arm, the amount of time spent in arms, and the time spent in the center square. After every animal, the testing apparatus was wiped down with 30–70% ethanol. Animals that spent a greater percentage of time in the closed arms were considered more anxious, whereas, conversely, animals that spent a greater percentage of time exploring the open arms were considered less anxious.

FGF9 Knockdown Studies.

shRNA and lentivirus construction. Three 19-mer siRNA sequences targeted against the coding region of the rat FGF9 mRNA sequence (accession number: NM_012952.1) were generated using an RNAi design site (Dharmacon). The target sites on the FGF9 mRNA and corresponding siRNA sequences were as follows: FGF9 siRNA1 (414–433; AGGAAAGACCACAGCCGAT), FGF9 siRNA2 (415–434; GGAAAGACCACAGCCGATT), and FGF9 siRNA3 (682–701; GGACCAGGACTAAACGGCA). shRNA sequences were generated by adding a nine-nucleotide loop sequence (UUCAAGAGA) and restriction enzyme sites; the shRNA constructs were then synthesized (Invitrogen) and subcloned into the pLentiLox3.7 lentiviral vector (https://www.addgene.org/11795/), which drives shRNA expression using a mouse U6 promoter and which contains an eGFP reporter tag under the control of a CMV promoter. All shRNA inserts were verified by sequencing. A control, nonsilencing shRNA (shNS) sequence was also used (14). shRNA3 was selected to be used in vivo because it was the most effective at reducing FGF9 expression in vitro and showed the least toxic effects on cultured cells (<10% cell death). The vector containing shRNA3 (hereafter referred to as shFGF9), as well as vector containing a shNS (14), were submitted to the University of Michigan Viral Vector core for lentivirus synthesis. The returned lentiviruses (100× concentration; LVshFGF9 and LVshNS) were used in FGF9 knockdown experiments in vivo.

Cell culture studies. COS7 cells were grown in HyClone DMEM/high glucose media (Fisher Scientific) with 10% FBS (Invitrogen) and gentamycin (10 μg/mL; Gibco). Twenty-four hours after plating at 100,000 cells per well (six-well plates), cells were transfected with the psiCHECK2 vector (Promega) containing a clone of rat FGF9 (bp 37–869 of 1,065 total length; encompasses entirety of the coding region; generated in-house) or FGF2 (14) at 20 ng/μL and, in some conditions, either siRNA or shRNA constructs to knock down expression of FGF9, FGF2, or the control, nonsilencing construct at 7 ng/μL (shNS) (14). Dharmafect Duo transfection reagent (Dharmacon) was used to facilitate the transfection. Twenty-four hours after transfection, cells were lysed using passive lysis buffer, and lysates were collected for analysis of knockdown efficacy. The psiCHECK2 vector housing the FGF9 clone enabled us to use a Dual Luciferase Assay (Promega) to assess knockdown efficacy in vitro. The FGF9 clone was inserted downstream of the *Renilla* luciferase reporter, allowing the creation of a fusion *Renilla-FGF9* mRNA, whereas expression of the independent *Firefly* luciferase gene was used to normalize the chemoluminescence readout across wells. Lysates were exposed to chemolumiscent reagents in the Dual Luciferase Assay according to the manufacturer's instructions, and the ratio of *Renilla/Firefly* chemoluminescence was used to assess efficacy of FGF9 knockdown for each siRNA/shRNA candidate in vitro.

Animals. All animals underwent microinjection surgery in one of two condition groups (LVshFGF9, LVshNS). Under isoflurane anesthesia and using standard stereotaxic protocols, a 33-gauge microinjector was lowered into each hippocampus (coordinates from bregma: A/P −5.0, M/L ±3.5, D/V −3.6–3.8). One microliter of lentivirus containing either a shRNA targeted against FGF9 (LVshFGF9) or a nonsilencing control sequence (LVshNS) was infused over 4 min, at the rate of 0.25 μL/min. Microinjectors were left in place for an additional 2 min and then slowly removed to allow the virus to diffuse into the hippocampus. Holes were filled with bone wax, and staples were used to close the wound. Standard analgesics were administered. We allowed 4 wk for recovery and integration of the viral load before proceeding with testing. Following the 4-wk recovery period, animals were subjected to behavioral testing (schema in Fig. S5*A*; testing previously described). Twenty-four hours after the last behavioral test, animals were killed. Brains were rapidly extracted and frozen in 2-methylbutane at −30 °C and stored at −80 °C until processing.

mRNA ISH. To understand the regulation of key FGF ligands and receptors after our experimental procedures, tissue was collected 24 h following the last behavioral task. All rats were killed by rapid decapitation, and their brains were removed, snap-frozen in 2-methylbutane, and stored at −80 °C until sectioned. Tissue was sectioned at −20 °C at 10 μm (n = 5–6/group for social defeat and FGF9 administration experiments, n = 10–14/group for knockdown experiments), sliced in series throughout the hippocampus, mounted on Superfrost Plus slides (Fisher Scientific), and returned to −80 °C until processing . Sections were taken every 200 μm through the hippocampus, and ISH methodology was performed as previously described in detail elsewhere (33). All in situ probes were synthesized in our laboratory, and exposure times were experimentally determined for optimal signal and are as follows: FGF2 (7 d), FGF9 (14–21 d), FGFR1 (7 d), and eGFP (7 d). The rat mRNA sequences used for generating probes was complimentary to the following RefSeq database numbers: FGF2 (NM_019395, 716–994), FGF9 (NM_012952, 661–880), FGFR1 (NM_024146, 320–977). All cDNA segments were extracted (Qiaquick Gel Extraction kit; Qiagen), subcloned in Bluescript SK (Stratagene), and confirmed by nucleotide sequencing. The probes were labeled in a reaction mixture of 1 μg of linearized plasmid, 1× transcription buffer (Epicentre Technologies), 125 μCi of 35S-labeled UTP, 125 μCi of 35-S labeled CTP, 150 μM ATP and GTP, 12.5 mM DTT, 1 μL RNase inhibitor, and 1.5 μL T7 or T3 RNA polymerase. After hybridizing the labeled probes to the sectioned tissue, sections were thoroughly washed and exposed to Kodak BioMax MR Scientific Imaging Film (Sigma Aldrich).

ISH Quantification. Radioactive signals were quantified using computer-assisted optical densitometry software, Scion Image (Scio Corporation), or ImageJ (National Institutes of Health). Expanded quantification methods were used for knockdown experiments, described below. For all other experiments, integrated optical densities were determined by outlining a subfield (CA1, CA2, CA3, and dentate gyrus) of the hippocampus on each hemisphere and were corrected for background plus 3.5× its SD. Only pixels with gray values exceeding the threshold were included in the analysis. Data from multiple sections per animal were averaged resulting in a mean for each animal and an average was taken for each group.

For quantification of sections from animals in the FGF9 knockdown study, we used a modified quantification approach to enable us to quantify expression of a gene target (e.g., FGF9, FGF2, or FGFR1) only where we saw concurrent expression of eGFP. This approach also facilitated careful analysis of hippocampal anatomy impacted by viral infection on an animal-by-animal basis, which we then used to create inclusion/exclusion criteria for the behavioral analyses. We digitally overlaid a transparent copy of the eGFP autoradiogram (from an adjacent section) on the image of the probe of interest then outlined only the region with eGFP expression to take measurements for the probe of interest. Because there was variability in infection spread, we chose to disregard area in calculating the quantified measurements for these experiments; therefore, we present the data in terms of average optical density (mean signal background).

eGFP autoradiograms were separately analyzed for the specific animal-by-animal infection pattern, and these data were used to define strict inclusion criteria for behavioral analysis. Animals in the knockdown study were only included in the final behavioral analysis if they showed robust expression of eGFP (the marker for successful viral infection) in the dentate gyrus of both hemispheres in at least four adjacent sections (≥800 μm) without additional eGFP labeling of other hippocampal or extrahippocampal structures. After exclusion, 8 animals were included in the shNS control group, whereas 10 animals were included in the shFGF9 group.

Immunohistochemistry. A separate cohort of animals (n = 4 animals per group; shNS, shFGF9) underwent the same surgical procedures as those described in the behavioral knockdown study. Three weeks after surgery, animals were transcardially perfused using 4% (vol/vol) PFA. Brains were removed and postfixed for 1 h in fresh 4% PFA and then transferred to 30% sucrose solution for 24–48 h. Brains were subsequently snap-frozen in 2-methylbutane and stored at −80 °C until sectioned. Tissue was sectioned at −15 °C at 45 μm, and free-floating

sections were stored in PBS at 4 °C until processing. Free-floating sections were rinsed three times in PBS and then blocked for 1 h at room temperature on an orbital shaker [blocking solution: 0.3% Triton × 100 (Sigma-Aldrich), 1% normal goat serum (Invitrogen), and 1% BSA (Fisher Scientific) in 0.1 mol/L phosphate buffer]. After blocking, sections were incubated overnight at room temperature on the orbital shaker in the blocking solution with the following primary antibodies: eGFP (chicken anti-GFP, 1:2,000; Abcam), NeuN (rabbit anti-NeuN, 1:300; Abcam), and GFAP (mouse anti-GFAP, 1:500; Millipore). After primary antibody incubation, sections were washed three times in PBS and then transferred to blocking solution with the following three secondary antibodies with conjugated fluorophores (AlexaFluor488 goat anti-chicken IgG, 1:200; AlexaFluor568 goat anti-rabbit IgG, 1:200; AlexaFluor 647 goat anti-mouse, 1:200; Life Technologies) to incubate for 2 h at room temperature on the orbital shaker. After secondary incubation, sections were washed four to five times in PBS and mounted onto Superfrost Plus slides and coverslipped using ProLong Gold Antifade Reagent with DAPI (Fisher Scientific). Slides were imaged on an Olympus Fluoview FV1000 confocal microscope with a multiline argon laser (457, 488, and 515 nm), 405-nm diode laser, and 543- and 633-nm HeNe lasers. Microscope control and image acquisition was achieved using Olympus FV10 software.

ACKNOWLEDGMENTS

We thank all the members of the Pritzker Consortium (especially the University of California, Irvine Brain Bank staff), and Robert Thompson, Juan Lopez, Adriana Medina, and David Krowleski for brain dissections. We also thank Audrey Seasholtz, Gwen Schaefer, Jack Parent, Hui Li, Jennifer Fitzpatrick, Jim Stewart, Fei Li, Amy Tang, Mary Hoversten, and Sharon Burke. This work was supported by the Pritzker Neuropsychiatric Research Consortium, Office of Naval Research Grants ONR N00014-15-1-2224 and ONR N00014-12-1-0366, National Institutes of Health Grant R01MH104261, and the Hope for Depression Research Foundation. E.L.A. was supported by National Science Foundation Graduate Research Fellowship Program and NIH Grants 5T32DA007281-17 and 5T32EY017878-10.

FOOTNOTES

Conflict of interest: E.L.A., C.A.T., M.H.H., J.Z.L., D.A., P.B., W.E.B., R.M.M., J.D.B., A.F.S., S.J.W., and H.A. are members of the Pritzker Neuropsychiatric Research Consortium, which is supported by the Pritzker Neuropsychatric Disorders Research Fund, LLC (Fund). There exists a shared intellectual property agreement between the academic and philanthropic entities of the Consortium. The Fund has no role in study design, data collection and analysis, decision to publish, or preparation of the manuscript.

This article contains supporting information online at www.pnas.org/lookup/suppl/doi:10.1073/pnas.1510456112/-/DCSupplemental.

ARTICLE INFORMATION

Proc Natl Acad Sci U S A. 2015 Sep 22; 112(38): 11953–11958.
Published online 2015 Sep 8. doi: 10.1073/pnas.1510456112
PMCID: PMC4586860
PMID: 26351673
Neuroscience

Elyse L. Aurbach,[a,b,1] Edny Gula Inui,[a,1] Cortney A. Turner,[a] Megan H. Hagenauer,[a] Katherine E. Prater,[a,b] Jun Z. Li,[a] Devin Absher,[c] Najmul Shah,[a] Peter Blandino, Jr.,[a] William E. Bunney,[c] Richard M. Myers,[d] Jack D. Barchas,[e] Alan F. Schatzberg,[f] Stanley J. Watson, Jr.,[a] and Huda Akil[a,2]

[a]Molecular and Behavioral Neuroscience Institute, University of Michigan, Ann Arbor, MI, 48109;
[b]Neuroscience Graduate Program, University of Michigan, Ann Arbor, MI, 48109;
[c]Department of Psychiatry & Human Behavior, University of California, Irvine, CA, 92697;
[d]HudsonAlpha Institute for Biotechnology, Huntsville, AL, 35806;
[e]Department of Psychiatry, Cornell University, New York, NY, 10065;
[f]Department of Psychiatry, Stanford University, Stanford, CA, 94305
[2]To whom correspondence should be addressed. Email: akil@umich.edu.
Contributed by Huda Akil, August 6, 2015 (sent for review July 21, 2015; reviewed by Victoria Arango and James P. Herman)

Author contributions: E.L.A., E.G.I., C.A.T., M.H.H., J.Z.L., W.E.B., R.M.M., J.D.B., A.F.S., S.J.W., and H.A. designed research; E.L.A., E.G.I., M.H.H., K.E.P., J.Z.L., D.A., N.S., R.M.M., and S.J.W. performed research; E.L.A., M.H.H., J.Z.L., D.A., P.B., W.E.B., R.M.M., J.D.B., A.F.S., and S.J.W. contributed new reagents/analytic tools; E.L.A.,

E.G.I., M.H.H., and K.E.P. analyzed data; E.L.A., E.G.I., C.A.T., M.H.H., K.E.P., and H.A. wrote the paper; C.A.T. provided coordination of the Pritzker Database; W.E.B. provided coordination, administration, and oversight of the Brain Bank; and R.M.M., J.D.B., A.F.S., and S.J.W. created the Consortium infrastructure for the human studies.

Reviewers: V.A., Columbia University; and J.P.H., University of Cincinnati.

[1]E.L.A. and E.G.I. contributed equally to this work.

REFERENCES

1. Turner CA, Watson SJ, Akil H. The fibroblast growth factor family: Neuromodulation of affective behavior. Neuron. 2012;76(1):160–174. [PMC free article] [PubMed]

2. Duman RS, Monteggia LM. A neurotrophic model for stress-related mood disorders. Biol Psychiatry. 2006;59(12):1116–1127. [PubMed]

3. Evans SJ, et al. Dysregulation of the fibroblast growth factor system in major depression. Proc Natl Acad Sci USA. 2004;101(43):15506–15511. [PMC free article] [PubMed]

4. Bernard R, et al. Altered expression of glutamate signaling, growth factor, and glia genes in the locus coeruleus of patients with major depression. Mol Psychiatry. 2011;16(6):634–646. [PMC free article] [PubMed]

5. Gaughran F, Payne J, Sedgwick PM, Cotter D, Berry M. Hippocampal FGF-2 and FGFR1 mRNA expression in major depression, schizophrenia and bipolar disorder. Brain Res Bull. 2006;70(3):221–227. [PubMed]

6. Turner CA, Calvo N, Frost DO, Akil H, Watson SJ. The fibroblast growth factor system is downregulated following social defeat. Neurosci Lett. 2008;430(2):147–150. [PMC free article] [PubMed]

7. Turner CA, Gula EL, Taylor LP, Watson SJ, Akil H. Antidepressant-like effects of intracerebroventricular FGF2 in rats. Brain Res. 2008;1224:63–68. [PMC free article] [PubMed]

8. Elsayed M, et al. Antidepressant effects of fibroblast growth factor-2 in behavioral and cellular models of depression. Biol Psychiatry. 2012;72(4):258–265. [PMC free article] [PubMed]

9. Mallei A, Shi B, Mocchetti I. Antidepressant treatments induce the expression of basic fibroblast growth factor in cortical and hippocampal neurons. Mol Pharmacol. 2002;61(5):1017–1024. [PubMed]

10. Bachis A, Mallei A, Cruz MI, Wellstein A, Mocchetti I. Chronic antidepressant treatments increase basic fibroblast growth factor and fibroblast growth factor-binding protein in neurons. Neuropharmacology. 2008;55(7):1114–1120. [PMC free article] [PubMed]

11. Gómez-Pinilla F, Dao L, Choi J, Ryba EA. Diazepam induces FGF-2 mRNA in the hippocampus and striatum. Brain Res Bull. 2000;53(3):283–289. [PubMed]

12. Perez JA, Clinton SM, Turner CA, Watson SJ, Akil H. A new role for FGF2 as an endogenous inhibitor of anxiety. J Neurosci. 2009;29(19):6379–6387. [PMC free article] [PubMed]

13. Turner CA, Clinton SM, Thompson RC, Watson SJ, Jr, Akil H. Fibroblast growth factor-2 (FGF2) augmentation early in life alters hippocampal development and rescues the anxiety phenotype in vulnerable animals. Proc Natl Acad Sci USA. 2011;108(19):8021–8025. [PMC free article] [PubMed]

14. Eren-Koçak E, Turner CA, Watson SJ, Akil H. Short-hairpin RNA silencing of endogenous fibroblast growth factor 2 in rat hippocampus increases anxiety behavior. Biol Psychiatry. 2011;69(6):534–540. [PMC free article] [PubMed]

15. Salaria S, et al. Microarray analysis of cultured human brain aggregates following cortisol exposure: Implications for cellular functions relevant to mood disorders. Neurobiol Dis. 2006;23(3):630–636. [PubMed]

16. Tagashira S, Ozaki K, Ohta M, Itoh N. Localization of fibroblast growth factor-9 mRNA in the rat brain. Brain Res Mol Brain Res. 1995;30(2):233–241. [PubMed]

17. Nakamura S, et al. Motor neurons in human and rat spinal cord synthesize fibroblast growth factor-9. Neurosci Lett. 1997;221(2-3):181–184. [PubMed]

18. Todo T, et al. Neuronal localization of fibroblast growth factor-9 immunoreactivity in human and rat brain. Brain Res. 1998;783(2):179–187. [PubMed]

19. Garcès A, Nishimune H, Philippe J-M, Pettmann B, deLapeyrière O. FGF9: A motoneuron survival factor expressed by medial thoracic and sacral motoneurons. J Neurosci Res. 2000;60(1):1–9. [PubMed]

20. Lin Y, et al. Neuron-derived FGF9 is essential for scaffold formation of Bergmann radial fibers and migration of granule neurons in the cerebellum. Dev Biol. 2009;329(1):44–54. [PMC free article] [PubMed]

21. Nakamura S, et al. Glial expression of fibroblast growth factor-9 in rat central nervous system. Glia. 1999;28(1):53–65. [PubMed]

22. Goetz R, Mohammadi M. Exploring mechanisms of FGF signalling through the lens of structural biology. Nat Rev Mol Cell Biol. 2013;14(3):166–180. [PMC free article] [PubMed]

23. Ornitz DM, et al. Receptor specificity of the fibroblast growth factor family. J Biol Chem. 1996;271(25):15292–15297. [PubMed]

24. Huang J-Y, Hong Y-T, Chuang J-I. Fibroblast growth factor 9 prevents MPP+-induced death of dopaminergic neurons and is involved in melatonin neuroprotection in vivo and in vitro. J Neurochem. 2009;109(5):1400–1412. [PubMed]

25. Kanda T, et al. Self-secretion of fibroblast growth factor-9 supports basal forebrain cholinergic neurons in an autocrine/paracrine manner. Brain Res. 2000;876(1-2):22–30. [PubMed]

26. Lum M, Turbic A, Mitrovic B, Turnley AM. Fibroblast growth factor-9 inhibits astrocyte differentiation of adult mouse neural progenitor cells. J Neurosci Res. 2009;87(10):2201–2210. [PubMed]

27. Li JZ, et al. Systematic changes in gene expression in postmortem human brains associated with tissue pH and terminal medical conditions. Hum Mol Genet. 2004;13(6):609–616. [PubMed]

28. Chaudhury S, et al. FGF2 is a target and a trigger of epigenetic mechanisms associated with differences in emotionality: Partnership with H3K9me3. Proc Natl Acad Sci USA. 2014;111(32):11834–11839. [PMC free article] [PubMed]

29. Lamers F, et al. Comorbidity patterns of anxiety and depressive disorders in a large cohort study: The Netherlands Study of Depression and Anxiety (NESDA) J Clin Psychiatry. 2011;72(3):341–348. [PubMed]

30. American Psychiatric Association (2000) *Diagnostic and Statistical Manual of Mental Disorders* (American Psychiatric Association, Washington, DC), 4th Ed.

31. Li JZ, et al. Circadian patterns of gene expression in the human brain and disruption in major depressive disorder. Proc Natl Acad Sci USA. 2013;110(24):9950–9955. [PMC free article] [PubMed]

32. Tomita H, et al. Effect of agonal and postmortem factors on gene expression profile: Quality control in microarray analyses of postmortem human brain. Biol Psychiatry. 2004;55(4):346–352. [PMC free article] [PubMed]

33. Livak KJ, Schmittgen TD. Analysis of relative gene expression data using real-time quantitative PCR and the 2(-Δ Δ C(T)) Method. Methods. 2001;25(4):402–408. [PubMed]

34. Kabbaj M, Devine DP, Savage VR, Akil H. Neurobiological correlates of individual differences in novelty-seeking behavior in the rat: Differential expression of stress-related molecules. J Neurosci. 2000;20(18):6983–6988. [PubMed]